Title

(n,p) ELASTIC SCATTERING: A FITTING EXPRESSION FOR THE DIFFERENTIAL CROSS SECTIONS IN THE ENERGY RANGE BETWEEN 22.5 AND 400 MeV

Authors

Rindi, Alessandro.
Lim, Chun Bin.
Salmon-Cinotti, Tullio.

Publication Date

1970-11-01

UCRL-20295 c.2
UC-34 Physics
TID-4500 (57th Ed.)

(n, p) ELASTIC SCATTERING: A FITTING EXPRESSION FOR THE DIFFERENTIAL CROSS SECTIONS IN THE ENERGY RANGE BETWEEN 22.5 AND 400 MeV

Alessandro Rindi, Chun Bin Lim, and
Tullio Salmon-Cinotti

November 20, 1970

AEC Contract No. W-7405-eng-48

LAWRENCE RADIATION LABORATORY
UNIVERSITY of CALIFORNIA BERKELEY

DISCLAIMER

(n, p) ELASTIC SCATTERING: A FITTING EXPRESSION FOR THE DIFFERENTIAL CROSS SECTIONS IN THE ENERGY RANGE BETWEEN 22.5 AND 400 MeV

Alessandro Rindi, Chun Bin Lim, and Tullio Salmon-Cinotti†

Lawrence Radiation Laboratory
University of California
Berkeley, California 94720

November 20, 1970

ABSTRACT

The differential cross sections for the (n, p) elastic scattering at energies where the scattering is no longer isotropic in the c. m. system (i. e. for energies higher than about 10 MeV) are very often required for measurements of neutron fluxes and spectra. Literature provides a good amount of experimental data, but no simple empirical formula has yet been proposed that allows one to calculate the values of this cross section at any energy and at any angle.

N. Metropolis[1] and J. Gammel[2] have proposed two semi-empirical formulas that fit the total (n, p) elastic scattering cross section with an acceptable approximation for, respectively, energies higher than 71 MeV and energies up to 71 MeV. Using these formulas, F. Hajnal[3] has proposed a rather sophisticated empirical expression for fitting the differential cross section data up to about 600 MeV.

Using a part of the Hajnal results, we have sought a simpler expression fitting the experimental data with a better approximation. This study is a part of the program of the development of a fast neutron spectrometer to be used in stray fields around high energy accelerators.

INTRODUCTION

We have applied the least-square method for finding the coefficients of a fitting function expressing the n-p differential elastic-scattering cross section as a function of the c. m. neutron scattering angle (θ) and the lab incoming neutron kinetic energy (T) up to 400 MeV.

The experimental data of differential n-p scattering cross sections used in our calculations were obtained from the Experimental Cross Section Information Library of the Lawrence Radiation Laboratory–Livermore.[4] Gammel[2] has proposed a fitting function for the n-p elastic differential cross section based on the assumption that it is symmetrical about 90 deg in the c. m. system; this function fits the experimental data rather nicely up to 42 MeV. It was used as the primary part of our fitting function. A $\cos^3\theta$ and a $\cos^4\theta$ term were added as suggested by Gammel. Then we tried the best fitting by adding also several sinusoidal terms: the best fitting up to 400 MeV was found by adding a $\sin\theta$, a $\sin 2\theta$, and a $\sin 4\theta$ term. The final expression we used is shown as Eq. 12.

In the least-square calculation of the coefficients of the fitting function, the condition was imposed that the differential cross sections should satisfy the total scattering cross section on integration over the whole solid angle. In our energy range essentially elastic scattering is the only mode of process.

Incidentally, there are many more experimental data for the total cross sections than for the differential cross sections, and semi-empirical fitting functions which approximate very accurately the total cross sections in our energy range have been proposed. Gammel's function[2] approximates the total cross section accurately up to 71 MeV, and Metropolis's formula[1] gives a good fit for the rest of our energy range, as shown in Fig. 1. These functions were used to supply the total cross section for each neutron energy in the actual calculation of the coefficients of the fitting formula for differential cross section. In fact, the calculational scheme was set up in such a way that it automatically satisfies this normalization to the above total cross section in applying the least-square method. This constraint sometimes causes a worsening of the fitting of the differential cross section, especially when the values of the total cross section as given by the functions are not in agreement with the corresponding experimental data. Each experimental datum of the differential cross section was given different weight: the inverse of the data value was used as weight.

For some energies there were so few experimental data that it was very difficult to find a good fitting shape. In those cases, some fake data points were inserted in the calculation to make the shape compatible with the currently accepted behavior. This was especially true for the low energy region, namely below 40 MeV. The fitting functions calculated according to the above method can be used to predict the differential cross sections at energies for which the experimental data are not available, using a simple linear interpolation.

II. CALCULATION METHOD

A. Least-Square Method

As is shown in the next section, our object is to represent the shape of (n-p) elastic scattering cross sections as a linear combination of several preselected sinusoidal functions, and the least-square method is used in the process of selecting the coefficients of these functions that give the minimum deviation between the experimental data and the fitting-function values at data points. The least-square method as used in our calculations[5] is as follows.

The least-square method assumes that the best approximation over a domain D, which is composed of N discrete points, is that one for which the sum of the squared errors in D is minimum. Suppose that the values of f(x) are experimentally known over a discrete set of N values $x_1 \cdots x_N$ of the variable x in an interval (a, b), and that the approximation function has the form

$$y(x_\alpha) \equiv \sum_{k=1}^{n} a_k \phi_k(x_\alpha) \approx f(x_\alpha) \qquad (\text{for } \alpha = 1, \cdots N), \quad (1)$$

where $\phi_k(x)$ are n appropriately chosen functions.

Let's suppose that each data point has different weight $w(x_\alpha)$. If we define for each of the N points the residual $R(x_\alpha)$ by the equation

$$R(x_\alpha) \equiv f(x_\alpha) - \sum_{k=1}^{n} a_k \phi_k(x_\alpha) = f(x_\alpha) - y(x_\alpha), \quad (2)$$

the best approximation, in the least-squares sense, is defined to be that for which the coefficients a are determined so that the sum of $w(x_\alpha)\, R^2(x_\alpha)$ over the N data points is minimum. If we write this sum as

$$\langle wR^2 \rangle_\alpha \equiv \sum_{\alpha=1}^{N} w(x_\alpha) \times \left[f(x_\alpha) - \sum_{k=1}^{n} a_k \phi_k(x_\alpha) \right]^2 = \min, \tag{3}$$

this imposes the conditions

$$\frac{\partial}{\partial a_r} \left\langle w \left[f - \sum_{k=1}^{n} a_k \phi_k \right]^2 \right\rangle_\alpha = 0 \quad (\text{for } r = 1, \cdots, n) \tag{4}$$

or

$$\left\langle w\phi_r \left[f - \sum_{k=1}^{n} a_k \phi_k \right] \right\rangle_\alpha = \langle w\phi_r (f-y) \rangle_\alpha = 0 \tag{5}$$

or

$$\sum_{k=1}^{n} a_k \langle w\phi_r \phi \rangle_\alpha = \langle w\phi_r f \rangle_\alpha \quad (\text{for } r = 1, \cdots n). \tag{6}$$

This leads (for each set of N points, and for each energy value) to n simultaneous linear equations in the n unknown parameters a_1, a_1, $\cdots$ a_n. Here, the values $f(x_\alpha)$ are assumed to be known over discrete data points. These simultaneous linear equations can be solved by usual standard techniques. If we write these simultaneous equations again in more direct form, they appear as

$$a_1 \left[\sum_{\alpha=1}^{N} w(x_\alpha)\phi_r(x_\alpha)\phi_1(x_\alpha) \right] + a_2 \left[\sum_{\alpha=1}^{N} w(x_\alpha)\phi_r(x_\alpha)\phi_2(x_\alpha) \right] + a_n \left[\sum_{\alpha=1}^{N} w(x_\alpha)\phi_r(x_\alpha)\phi_n(x_\alpha) \right] = \left[\sum_{\alpha=1}^{N} w(x_\alpha)\phi_r(x_\alpha) f(x_\alpha) \right] \quad (\text{for } r = 1, \cdots n). \tag{7}$$

If we define an $n \times n$ matrix $\vec{K}$ by

$$\vec{K} = (K_{ij}) = \left[\sum_{\alpha=1}^{N} w(x_\alpha)\phi_i(x_\alpha)\phi_j(x_\alpha) \right] \tag{8}$$

and two column vectors $\vec{A}$ and $\vec{F}$ by

$$\vec{A} = \begin{bmatrix} a_1 \\ \cdot \\ \cdot \\ \cdot \\ a_n \end{bmatrix} \quad \vec{F} = \begin{bmatrix} f_1 \\ \cdot \\ \cdot \\ \cdot \\ f_n \end{bmatrix},$$

where $(f_i) = \left[\sum_{\alpha=1}^{N} w(x_\alpha)\phi_i(x_\alpha) f(x_\alpha) \right]$, (9)

the above equation becomes, in matrix form,

$$\vec{K} \times \vec{A} = \vec{F}. \tag{10}$$

Therefore if $\vec{K}$ is nonsingular, the solution vector $\vec{A}$ is

$$\vec{A} = (\vec{K})^{-1} \vec{F}. \tag{11}$$

In inverting the matrix $\vec{K}$, the LRL computer library subroutine LINIT was used.

B. Cross Section Expressions

In finding the functions for fitting the n-p elastic scattering cross sections to the experimental data, the following function was used for the c. m. system,

$$\sigma(\theta, T) = \frac{\sigma_{tot}(T)}{4\pi}\left[A\left(\frac{1+2\left(\frac{T}{90}\right)^2\cos^2\theta}{1+\frac{2}{3}\left(\frac{T}{90}\right)^2}\right) + B(\cos^3\theta) + C(\cos^4\theta) + D(\sin\theta) + E(\sin 2\theta) + F(\sin 4\theta) + G\right], \quad (12)$$

where θ is the neutron scattering angle in the c. m. system, in mb/sr, T is the kinetic energy of the incident neutron (in MeV) in the laboratory system, and A through G are the parameters to be determined. The above form was adapted to make it satisfy automatically the total scattering cross section when integrated over the whole solid angle.

The followings are the Gammel and Metropolis formulas for total scattering cross sections, respectively:

$$\sigma_G(T) = \left[\frac{3\pi}{1.206\,T + (-1.86 + 0.09415\,T + 0.0001306\,T^2)^2} + \frac{\pi}{1.206\,T + (0.4223 + 0.13\,T)^2}\right] \text{ in barns}, \quad (13)$$

and

$$\sigma_M(T) = \frac{34.10}{\beta^2} - \frac{82.2}{\beta} + 82.2 \text{ in mb}, \quad (14)$$

where $\beta = \frac{v}{c}$ is the neutron velocity in the laboratory system in c units. These formulas are plotted in Fig. 1 together with experimental data.

The requirement of normalization to the total scattering cross section at each incident neutron energy gives rise to a correlation between the coefficients.

Since

$$\int_0^{2\pi} d\phi \int_0^{\pi} \frac{1+2\,(T/90)^2\cos^2\theta}{1+(2/3)(T/90)^2} \sin\theta\, d\theta = 4\pi,$$

$$\int_0^{2\pi} d\phi \int_0^{\pi} \cos^3\theta \sin\theta\, d\theta = 0,$$

$$\int_0^{2\pi} d\phi \int_0^{\pi} \cos^4\theta \sin\theta\, d\theta = \frac{4\pi}{5},$$

$$\int_0^{2\pi} d\phi \int_0^{\pi} \sin\theta \sin\theta\, d\theta = \pi^2,$$

$$\int_0^{2\pi} d\phi \int_0^{\pi} \sin 2\theta \sin\theta\, d\theta = 0,$$

$$\int_0^{2\pi} d\phi \int_0^{\pi} \sin 4\theta \sin\theta\, d\theta = 0,$$

and

$$\int_0^{2\pi} d\phi \int_0^{\pi} 1 \sin\theta\, d\theta = 4\pi,$$

the integration of Eq. 12 gives

$$\sigma_{tot}(T) \equiv \int_{4\pi} \sigma(\theta, T)\, d\Omega = \frac{\sigma_{tot}(T)}{4\pi} \times \left(4\pi A + \frac{4\pi}{5} C + \pi^2 D + 4\pi G\right), \quad (15)$$

or

$$A = 1 - G - \frac{C}{5} - \left(\frac{\pi}{4}\right) D. \quad (16)$$

If we insert this relation in Eq. 12, we get

$$\sigma(\theta, T) - \frac{\sigma_{tot}(T)}{4\pi} \times g(\theta, T) = \frac{\sigma_{tot}(T)}{4\pi}$$

$$\times \left\{ B(\cos^3\theta) + C\left[\cos^4\theta - \frac{g(\theta, T)}{5}\right] \right.$$

$$+ D\left[\sin\theta - \frac{\pi}{4} g(\theta, T)\right] + E(\sin 2\theta)$$

$$\left. + F \sin 4\theta + G\left[1 - g(\theta, T)\right] \right\}, \qquad (17)$$

where

$$g(\theta, T) = \frac{1 + 2(T/90)^2 \cos^2\theta}{1 + 2/3 (T/90)^2} .$$

It is this equation that is used in the least-square calculation. Using the symbols of Section IIA, we have, for the neutron energy T,

$$f(\theta) = \sigma(\theta, T) - \frac{\sigma_{tot}(T)}{4\pi} g(\theta, T) ,$$

$$a_1 = B ; \quad \phi_1(\theta) = \cos^3\theta,$$

$$a_2 = C ; \quad \phi_2(\theta) = \cos^4\theta - \frac{1}{5} g(\theta, T),$$

$$a_3 = D ; \quad \phi_3(\theta) = \sin\theta - \frac{\pi}{4} g(\theta, T),$$

$$a_4 = E ; \quad \phi_4(\theta) = \sin 2\theta,$$

$$a_5 = F ; \quad \phi_5(\theta) = \sin 4\theta,$$

$$a_6 = G ; \quad \phi_6(\theta) = 1 - g(\theta, T),$$

and the matrix elements of $\vec{K}$ and $\vec{F}$ are

$$(K_{ij}) = \left[\sum_{\alpha=1}^{N} w(x_\alpha) \phi_i(x_\alpha) \phi_j(x_\alpha) , \right] ,$$

$$(f_i) = \left[\sum_{\alpha=1}^{N} w(x_\alpha) f(x_\alpha) \phi_i(x_\alpha) \right].$$

Then, the matrix equation for unknown matrix vector $\vec{A}$ is

$$\vec{K}\,\vec{A} = \vec{F},$$

and this was solved by using the LRL computer library subroutine LINIT, which was coded based on the Crout reduction technique. A system of linear equations is solved for each value of the neutron energy. Because not all the provided experimental data have error bars, the weight of each datum has been taken as the inverse of the datum itself.

III. RESULTS

In Table I are the calculated values of the seven constants of Eq. 12 for the different energies. In Fig. 1 we show the total cross section following the Gammel formula and the Metropolis formula together with the experimental data.

In Figs. 2 through 29 are plotted for the energy values for which we had experimental data, the Eq. (12) using the values of the constants tabulated in Table I, together with the experimental data. Some of the reported error bars on the experimental data which were not given in Ref. 4 have been taken from Ref. 6. The fitting of the formula varies with the energies. We calculated the goodness of the fit with the χ^2 method for each value of the energy.

We have plotted the values of the calculated differential cross-sections as a function of the energy for some angle of scattering by connecting the calculated points (at the energy values for which we had the coefficient) with a straight line. They are shown in Figs. 30 to 36. With the exception of those at 0 and 180 deg where the experimental values show large errors, these curves look quite smooth.

We use a linear interpolation between adjacent energy values for finding the cross sections for the energy values for which there is no experimental data. In Figs. 37 to 40 we show some cross section shapes for some energy values as calculated by linear interpolation.

ACKNOWLEDGMENTS

The authors express their gratitude to H. Wade Patterson for supporting, encouraging, and helping the project of the neutron spectrometer. T. Salmon-Cinotti, in particular, is very grateful to Dr. Patterson for allowing him to spend three months with the LRL Health Physics Group, and to all the members of the Health Physics Group and the 6600 Computer crew for the help they provided him.

FOOTNOTES AND REFERENCES

*Work done under auspices of the U. S. Atomic Energy Commission.

†Visiting student from the University of Bologna, Italy.

1. N. Metropolis, et al., Phys. Rev. 110, 185 (1958).

2. J. L. Gammel, The n-p Total and Differential Cross Section in Energy Range 0 to 40 MeV, from Fast Neutron Physics, Part II Eds. J. B. Marion and J. L. Fowler (Interscience, New York, 1963), p. 2185.

3. F. Hajnal, Relativistic n-p Scattering Calculations for Recoil Proton Spectrometers, Health and Safety Laboratory report, USAEC New York, October 1967.

4. T. Perkins, LRL-Livermore, provided us with the computer cards with the experimental values of the differential cross sections. The general code for the retrieval of the cross section is described in R. T. Howerton, et al., An Integrated System for Production of Neutronics and Photonic Calculation Constants, UCRL-50400 Vol. I Rev. 1, Feb. 1969. The data are supposed to be the same as those obtainable from the SIGMA Center of BNL.

5. F. B. Hildebrand, Introduction to Numerical Analysis (McGraw-Hill, New York, 1956).

6. M. H. McGregor, R. A. Arndt, and R. M. Wright, (p, p) and (n, p) Data Listing 0-750 MeV, Lawrence Radiation Laboratory report UCRL-50426, April 1968.

Table I. Fitting formula coefficients for the c. m. differential scattering cross sections.

T(MEV)	A	B	C	D	E	F	G
22.5	8.799E-01	-1.481E-02	-6.651E-02	0.	0.	0.	1.334E-01
27.5	-7.428E-01	3.215E-02	1.666E-01	0.	0.	0.	1.709E+00
28.4	-4.987E-01	-3.694E-02	1.819E-01	0.	0.	0.	1.462E+00
32.5	6.528E-01	-1.332E-02	1.188E-01	6.795E-02	7.297E-02	-1.095E-02	2.701E-01
37.5	4.375E-01	2.157E-03	-2.839E-01	-4.506E-01	5.698E-02	-1.081E-02	9.732E-01
42.5	8.902E-01	3.437E-02	-6.942E-01	-8.363E-01	2.629E-02	1.916E-02	9.055E-01
47.5	3.307E-01	4.451E-02	9.322E-02	-2.336E-01	3.064E-02	2.292E-02	8.342E-01
52.5	-8.409E-02	5.159E-02	5.668E-01	-9.561E-02	1.518E-02	1.756E-04	1.046E+00
57.5	-4.460E-02	5.211E-02	7.227E-01	-1.138E-02	2.665E-02	-1.237E-02	9.090E-01
62.5	4.536E-01	5.194E-02	4.514E-01	1.611E-02	1.599E-02	7.504E-02	4.434E-01
70.0	4.336E-01	-4.610E-02	2.084E-01	-5.318E-01	9.802E-02	4.248E-02	9.424E-01
80.0	3.107E-01	-1.775E-02	-5.047E-01	-1.313E+00	4.404E-02	-4.296E-02	1.822E+00
91.0	2.585E-01	-7.040E-02	-5.259E-01	-1.665E+00	-6.674E-04	5.871E-02	2.155E+00
99.0	6.168E-01	-2.012E-01	-6.357E-01	-1.297E+00	-8.475E-03	6.285E-02	1.529E+00
105.0	3.095E-01	-1.003E-01	-9.398E-01	-2.252E+00	-8.379E-03	1.009E-01	2.648E+00
108.5	3.262E-01	-1.377E-01	-8.891E-01	-2.118E+00	-1.181E-01	2.838E-02	2.515E+00
120.0	7.326E-02	-1.617E-01	7.956E-01	-7.141E-01	3.930E-02	3.708E-02	1.328E+00
130.0	-3.386E-01	-4.356E-01	-3.325E-02	-2.592E+00	-4.518E-02	8.249E-02	3.381E+00
137.0	2.200E-01	-1.891E-01	5.893E-01	-6.526E-01	-2.426E-01	-1.331E-02	1.175E+00
150.0	-2.312E-02	-1.521E-01	-1.094E-01	-2.412E+00	-1.069E-02	1.039E-01	2.939E+00
156.0	-7.533E-02	-5.355E-02	1.018E-02	-2.160E+00	-2.362E-01	2.060E-02	2.770E+00
172.0	-1.412E+00	-5.626E-01	5.776E-01	-5.753E+00	3.887E-01	2.147E-01	6.815E+00
200.0	-9.141E-01	-1.679E-01	-1.199E+00	-6.170E+00	-1.554E-01	-2.006E-02	7.000E+00
215.0	-7.336E-01	-1.177E-01	-9.291E-01	-6.365E+00	1.031E-02	3.960E-02	6.918E+00
260.0	-1.055E+00	1.886E-01	-2.946E-01	-6.667E+00	-2.046E-01	-4.154E-02	7.349E+00
300.0	-3.204E-01	-8.375E-01	-1.796E+00	-4.872E+00	3.462E-01	1.572E-01	5.506E+00
380.0	-1.485E+00	5.832E-03	-1.417E+00	-9.114E+00	-3.569E-02	-4.361E-02	9.926E+00
400.0	-7.619E-01	-9.052E-01	-3.060E+00	-8.174E+00	4.112E-01	1.377E-01	8.794E+00
580.0	-7.528E-01	2.333E-01	-1.544E+00	-7.034E+00	2.673E-01	-5.861E-02	7.586E+00
630.0	-9.030E-01	7.137E-01	-1.528E+00	-7.732E+00	-5.974E-02	-1.524E-01	8.281E+00

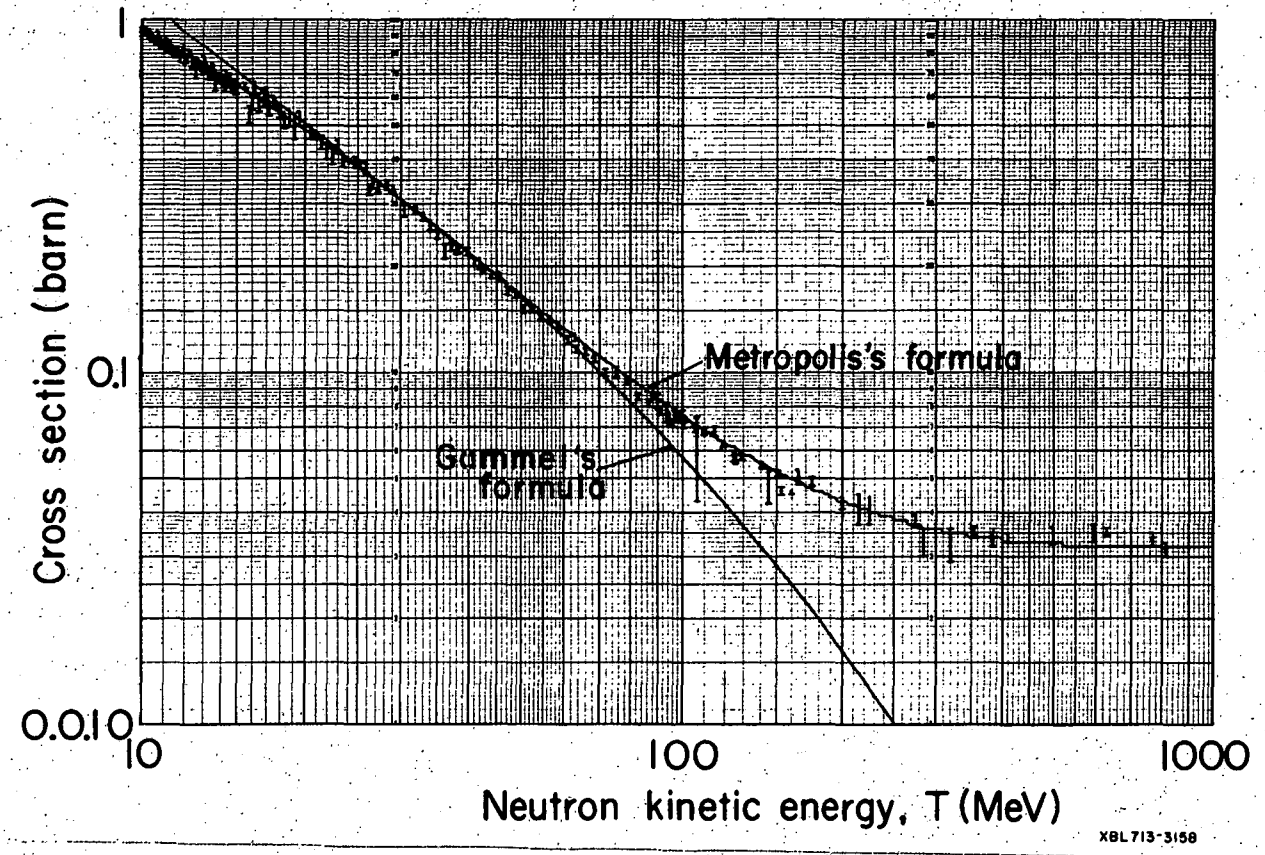

Fig. 1. Comparison of total n-p scattering cross sections calculated from Gammel's and Metropolis's formulas with experimental data.

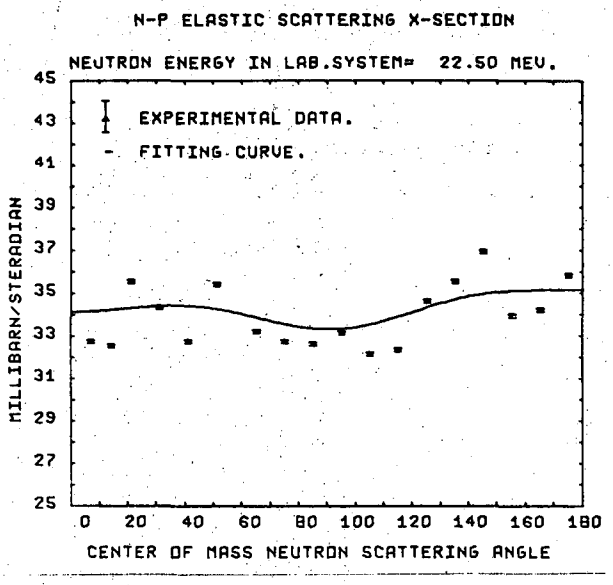

Fig. 2. Experimental data and fitting curves for np elastic scattering cross sections at various energies.

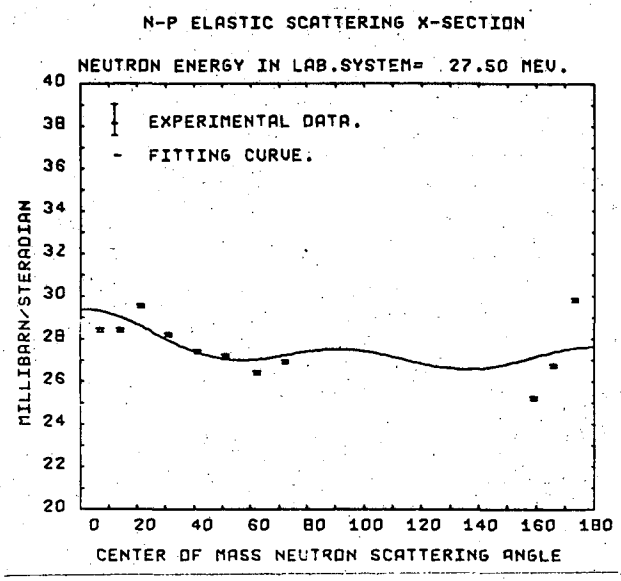

Fig. 3. Experimental data and fitting curves for np elastic scattering cross sections at various energies.

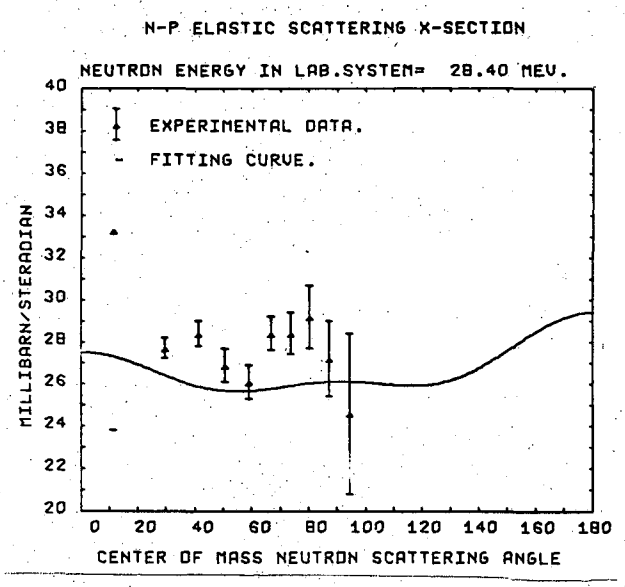

Fig. 4. Experimental data and fitting curves for np elastic scattering cross sections at various energies.

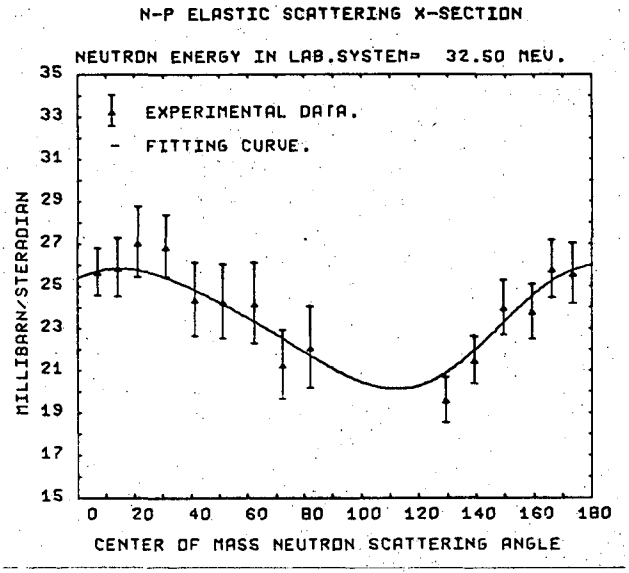

Fig. 5. Experimental data and fitting curves for np elastic scattering cross sections at various energies.

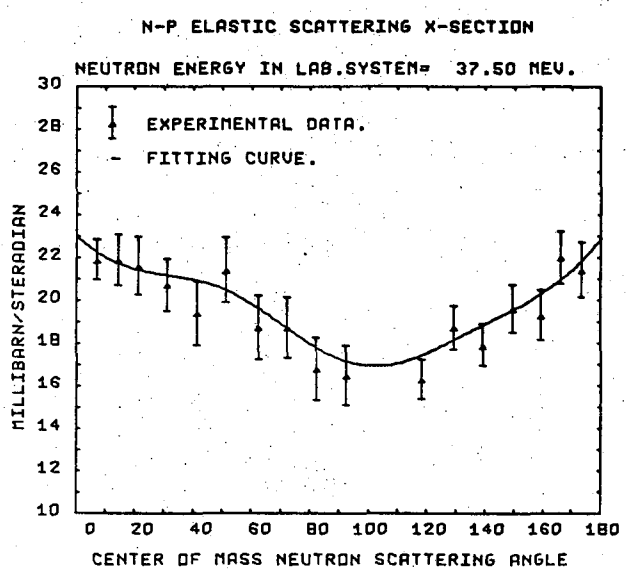

Fig. 6. Experimental data and fitting curves for np elastic scattering cross sections at various energies.

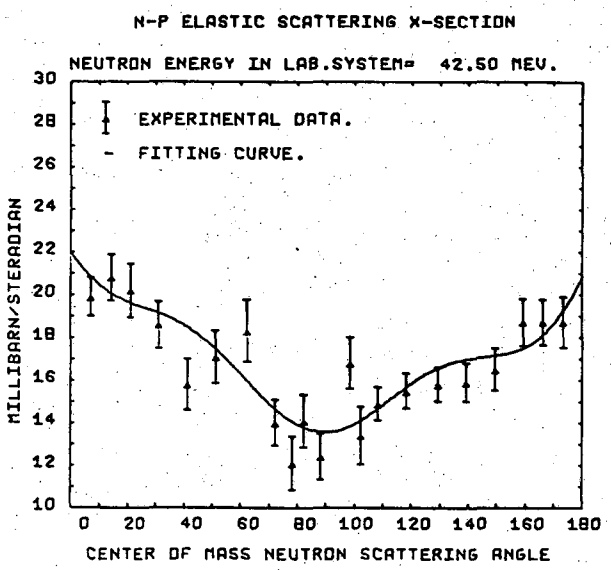

Fig. 7. Experimental data and fitting curves for np elastic scattering cross sections at various energies.

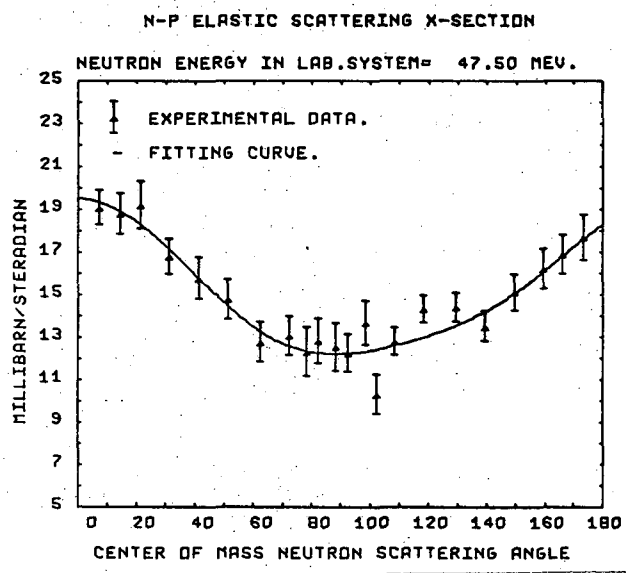

Fig. 8. Experimental data and fitting curves for np elastic scattering cross sections at various energies.

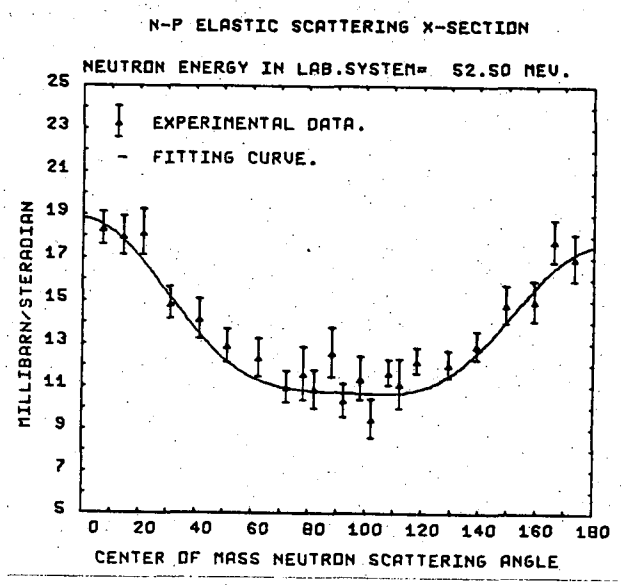

Fig. 9. Experimental data and fitting curves for np elastic scattering cross sections at various energies.

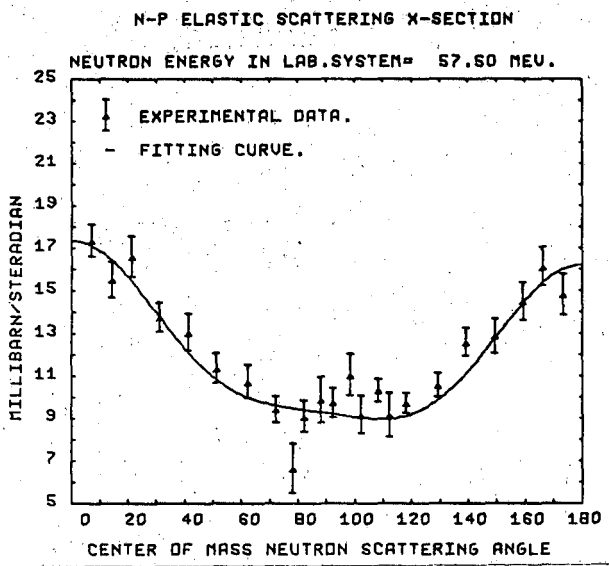

Fig. 10. Experimental data and fitting curves for np elastic scattering cross sections at various energies.

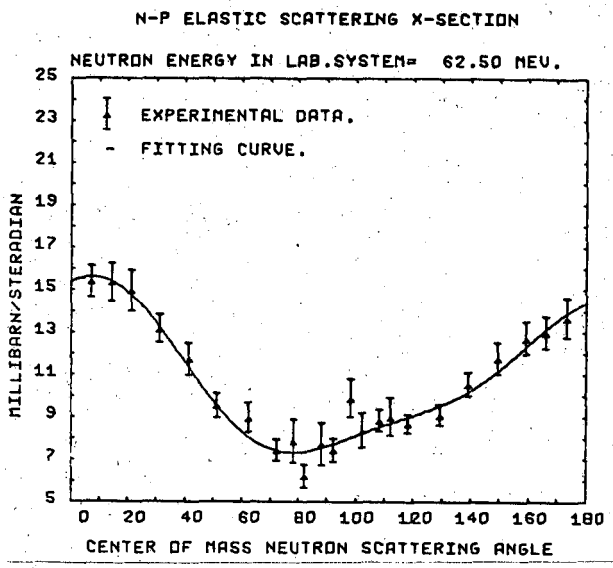

Fig. 11. Experimental data and fitting curves for np elastic scattering cross sections at various energies.

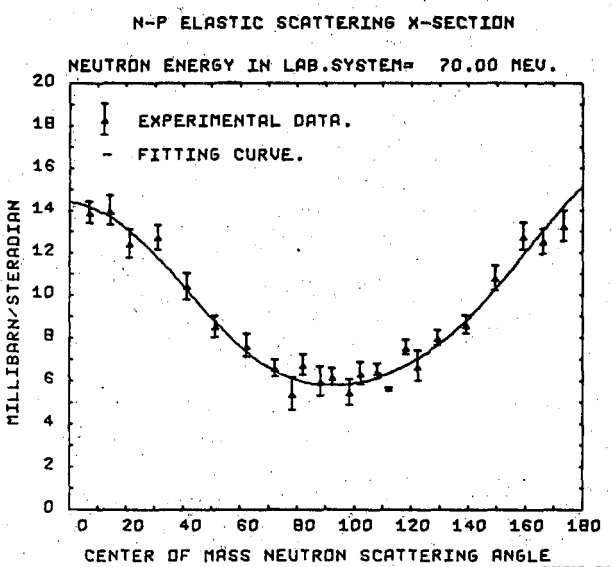

Fig. 12. Experimental data and fitting curves for np elastic scattering cross sections at various energies.

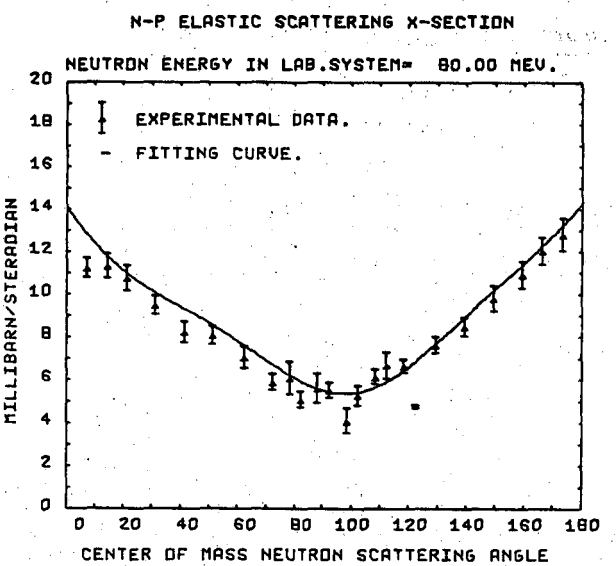

Fig. 13. Experimental data and fitting curves for np elastic scattering cross sections at various energies.

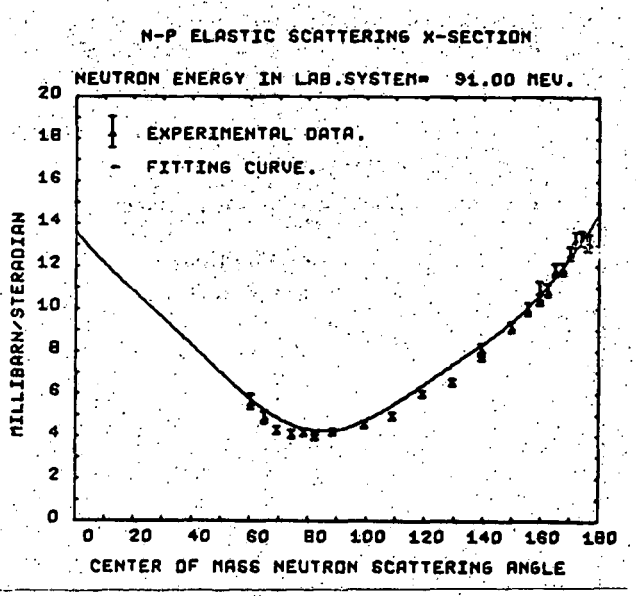

Fig. 14. Experimental data and fitting curves for np elastic scattering cross sections at various energies.

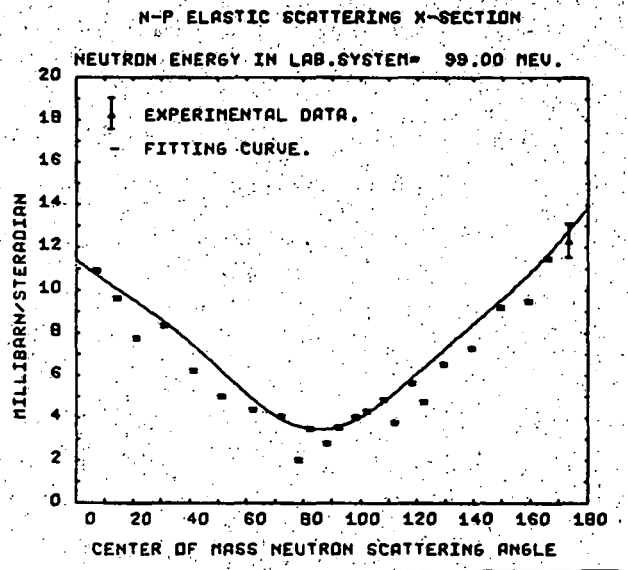

Fig. 15. Experimental data and fitting curves for np elastic scattering cross sections at various energies.

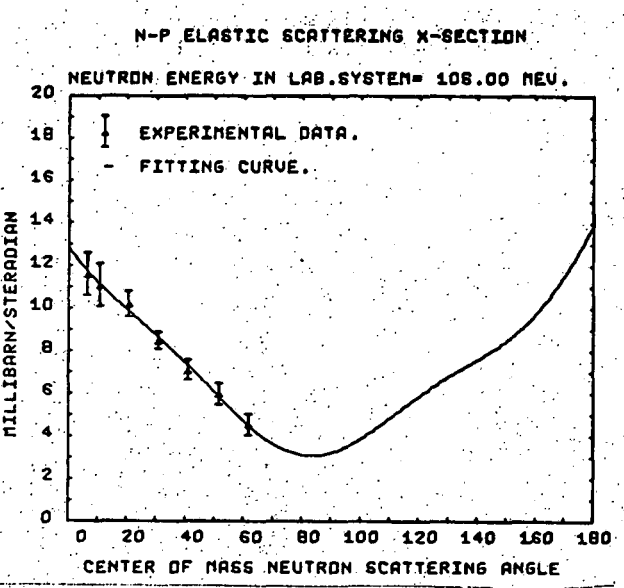

Fig. 16. Experimental data and fitting curves for np elastic scattering cross sections at various energies.

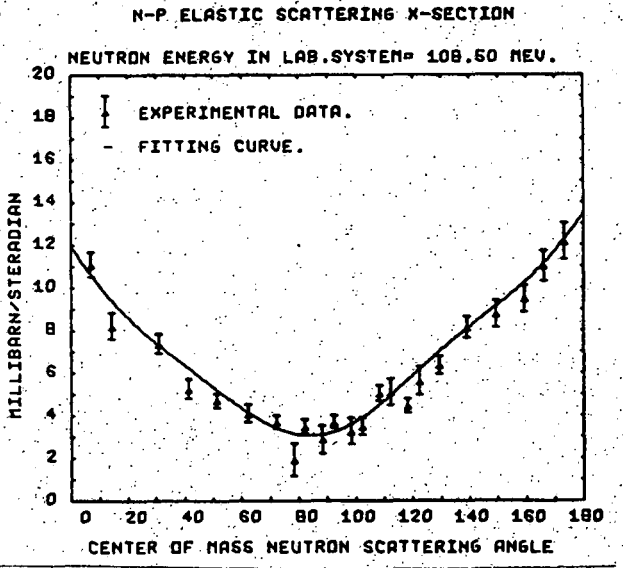

Fig. 17. Experimental data and fitting curves for np elastic scattering cross sections at various energies.

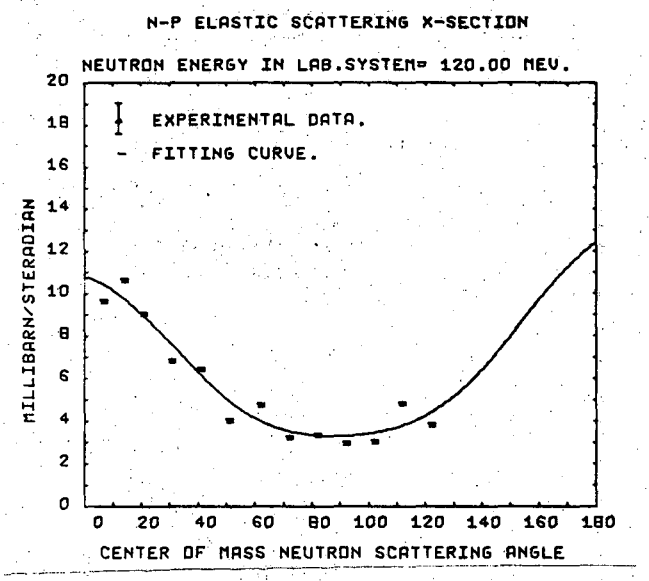

Fig. 18. Experimental data and fitting curves for np elastic scattering cross sections at various energies.

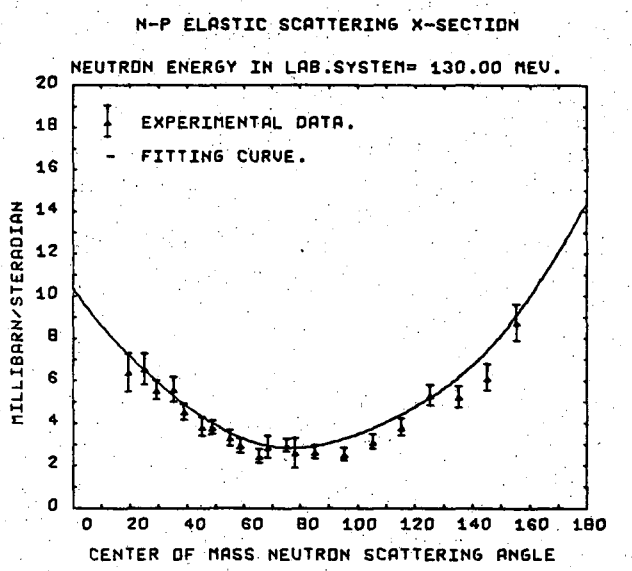

Fig. 19. Experimental data and fitting curves for np elastic scattering cross sections at various energies.

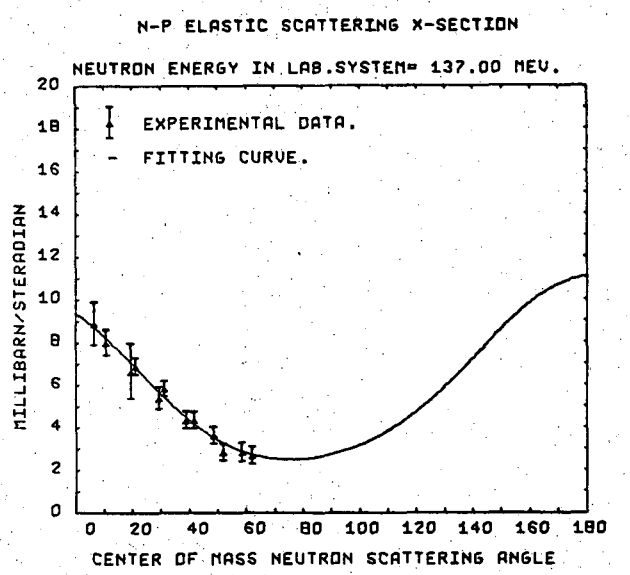

Fig. 20. Experimental data and fitting curves for np elastic scattering cross sections at various energies.

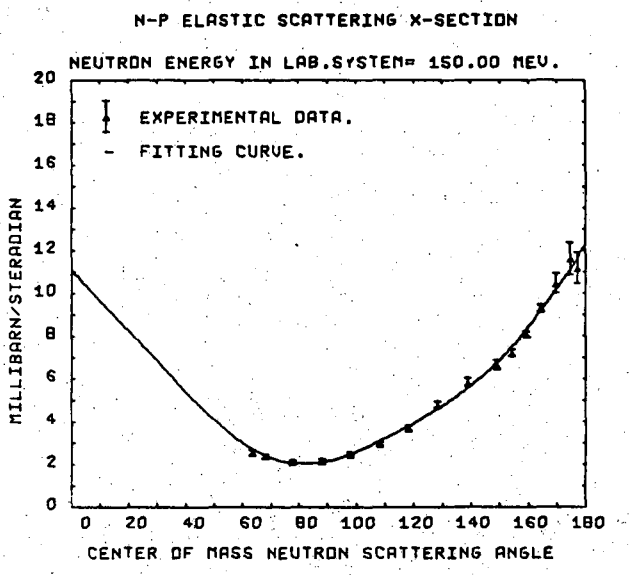

Fig. 21. Experimental data and fitting curves for np elastic scattering cross sections at various energies.

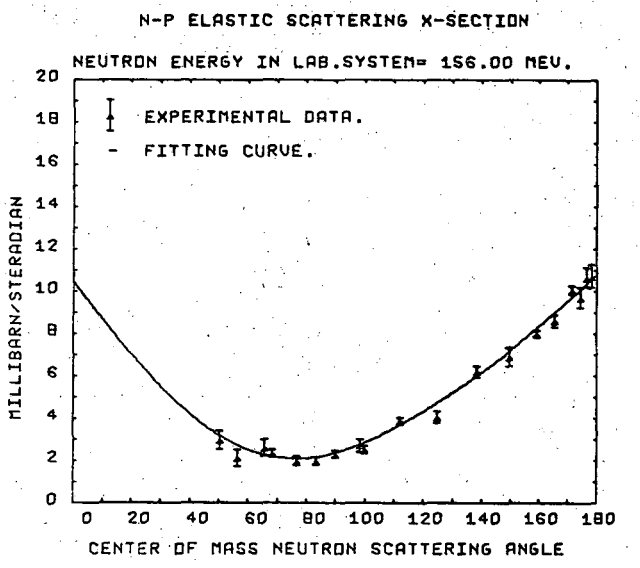

Fig. 22. Experimental data and fitting curves for np elastic scattering cross sections at various energies.

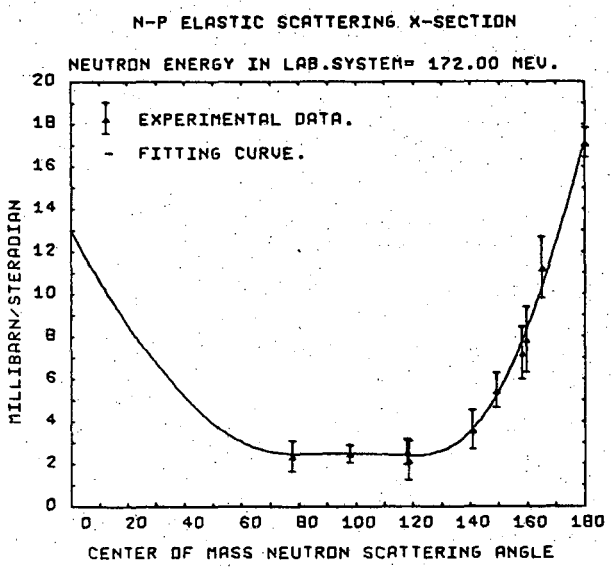

Fig. 23. Experimental data and fitting curves for np elastic scattering cross sections at various energies.

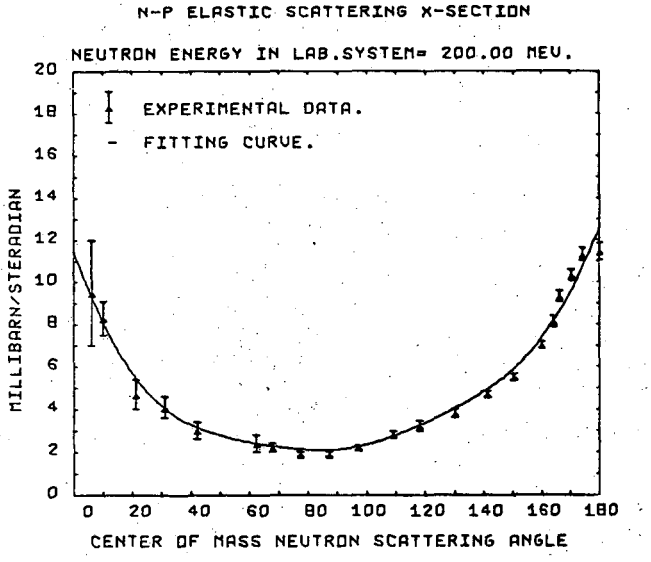

Fig. 24. Experimental data and fitting curves for np elastic scattering cross sections at various energies.

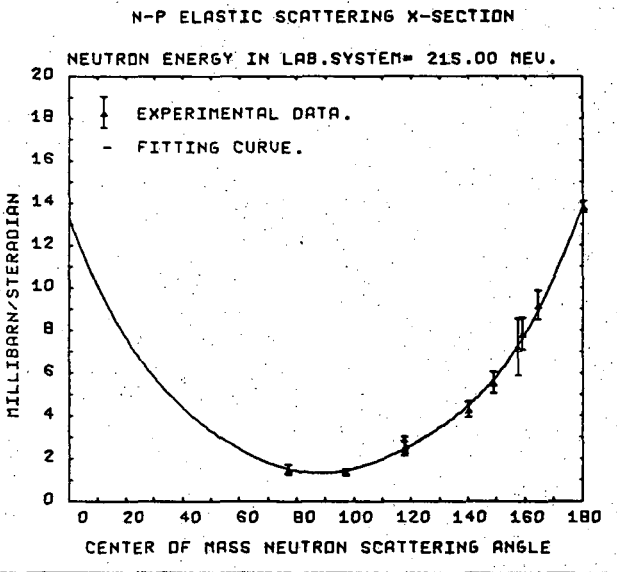

Fig. 25. Experimental data and fitting curves for np elastic scattering cross sections at various energies.

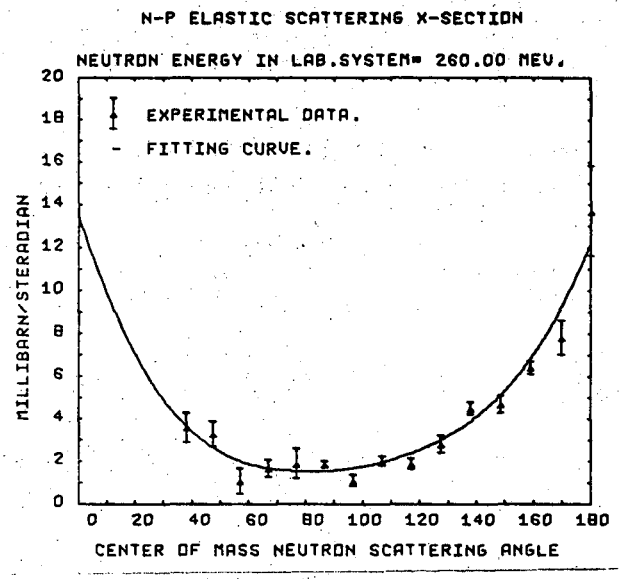

Fig. 26. Experimental data and fitting curves for np elastic scattering cross sections at various energies.

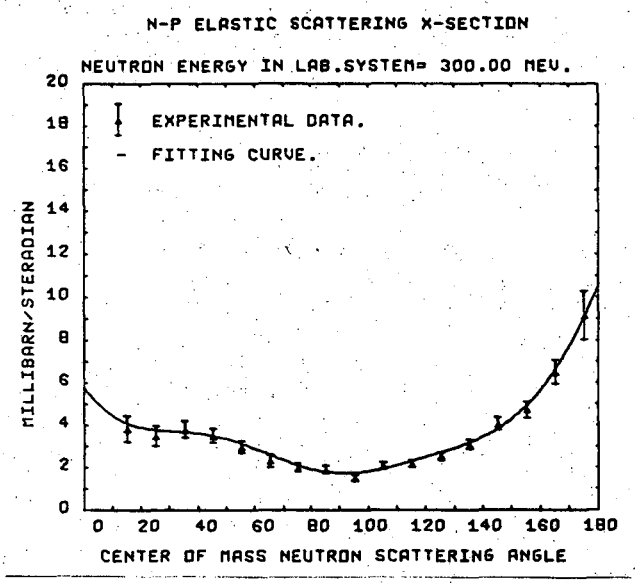

Fig. 27. Experimental data and fitting curves for np elastic scattering cross sections at various energies.

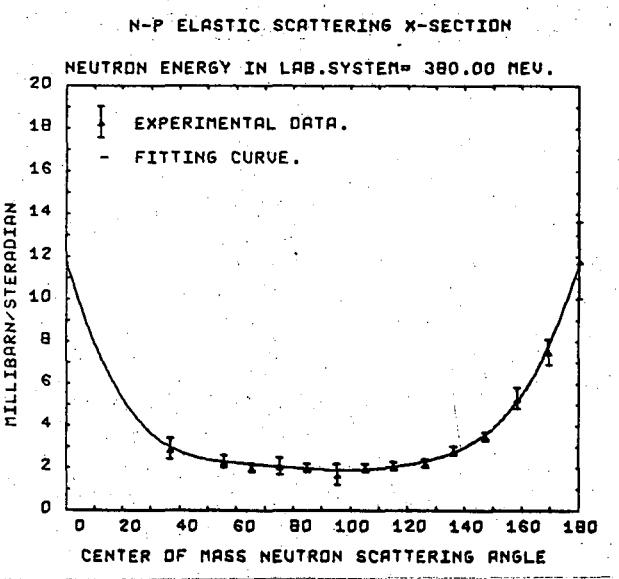

Fig. 28. Experimental data and fitting curves for np elastic scattering cross sections at various energies.

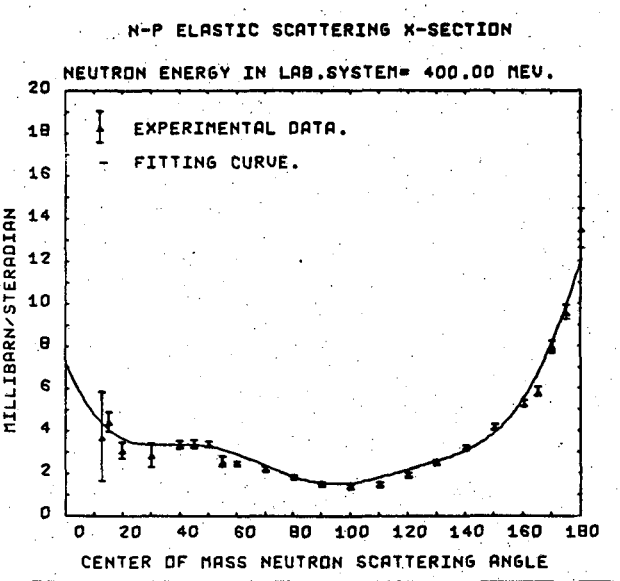

Fig. 29. Experimental data and fitting curves for np elastic scattering cross sections at various energies.

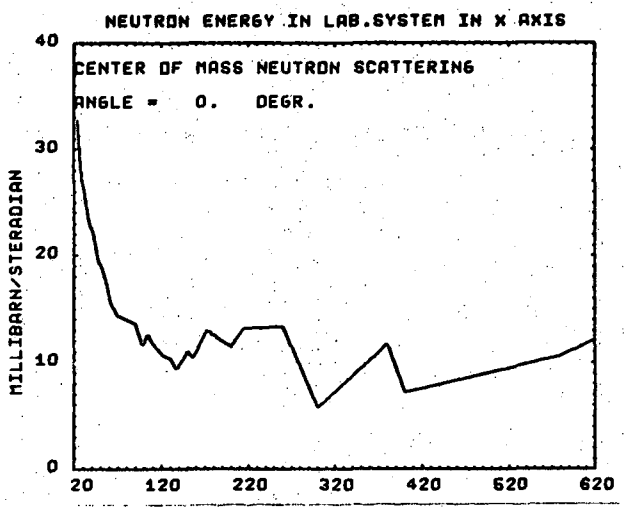

Fig. 30. Variation of cross section as a function of energy for various scattering angles.

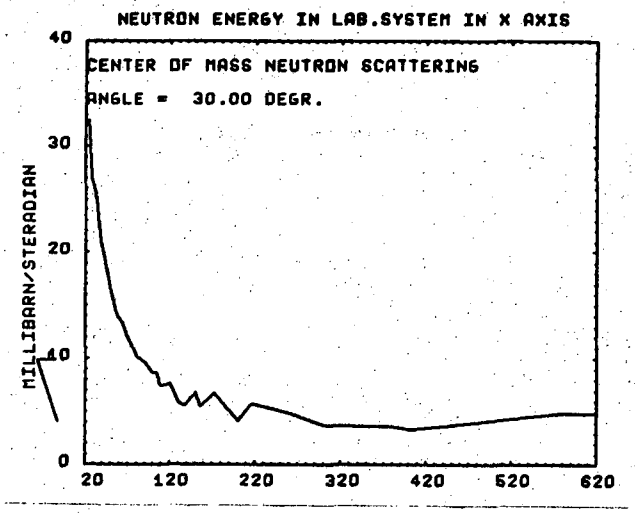

Fig. 31. Variation of cross section as a function of energy for various scattering angles.

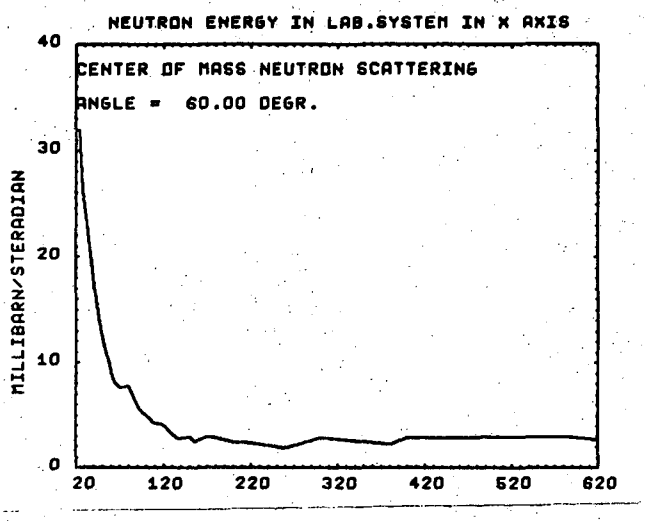

Fig. 32. Variation of cross section as a function of energy for various scattering angles.

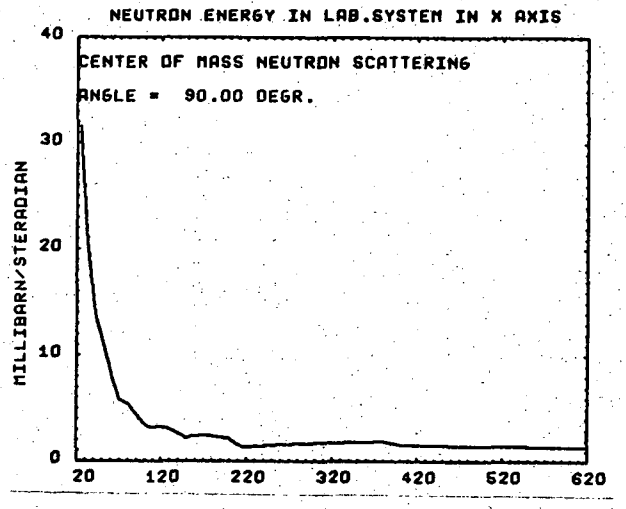

Fig. 33. Variation of cross section as a function of energy for various scattering angles.

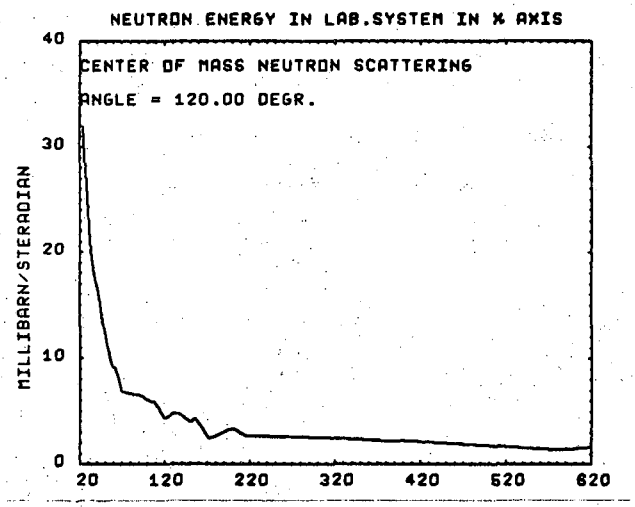

Fig. 34. Variation of cross section as a function of energy for various scattering angles.

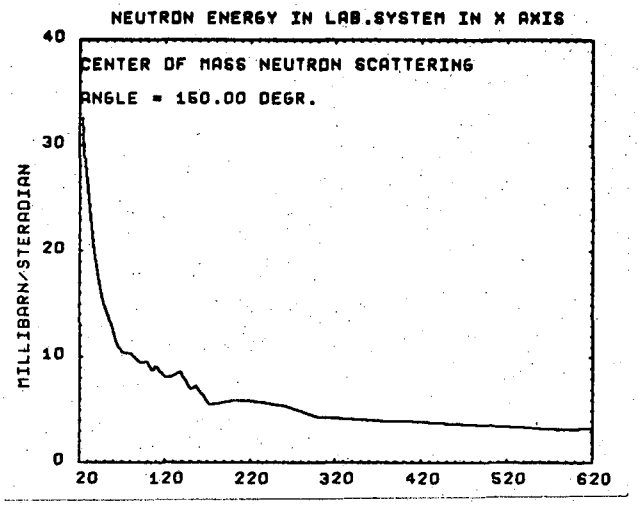

Fig. 35. Variation of cross section as a function of energy for various scattering angles.

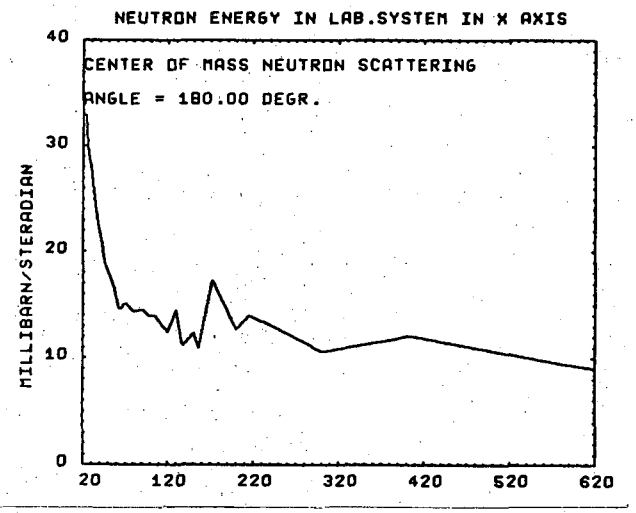

Fig. 36. Variation of cross section as a function of energy for various scattering angles.

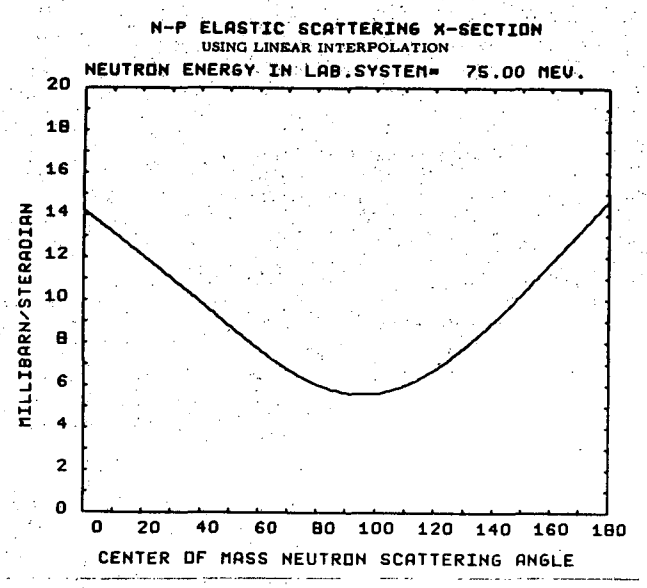

Fig. 37. Some examples of calculated np elastic scattering cross sections at some energies for which there are no experimental data.

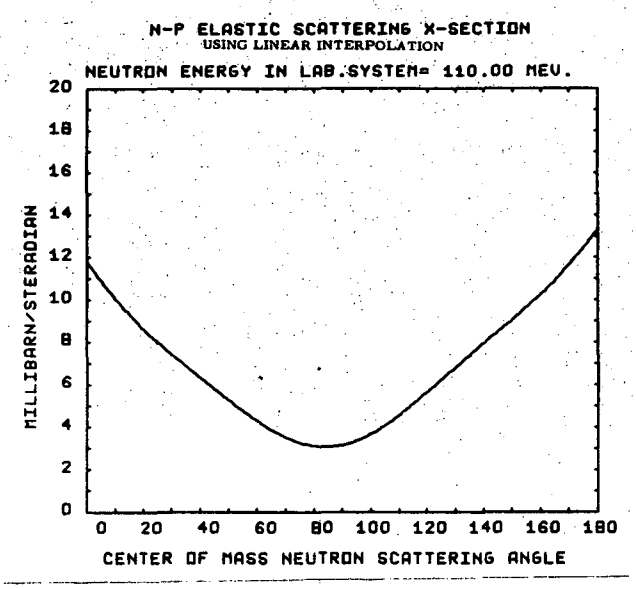

Fig. 38. Some examples of calculated np elastic scattering cross sections at some energies for which there are no experimental data.

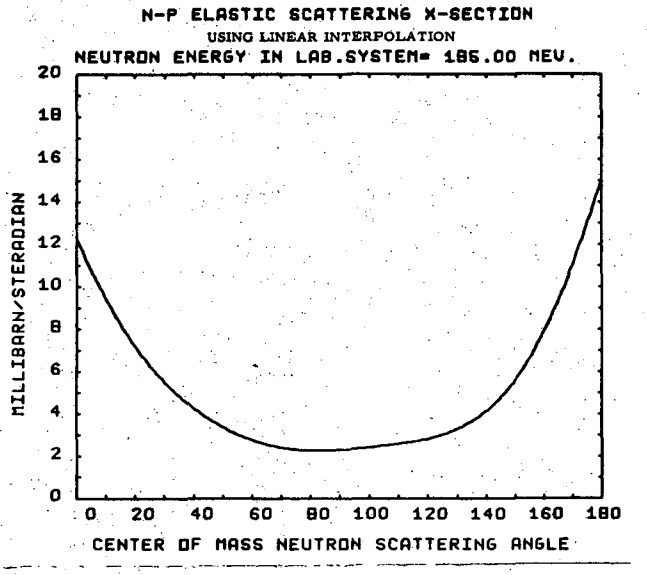

Fig. 39. Some examples of calculated np elastic scattering cross sections at some energies for which there are no experimental data.

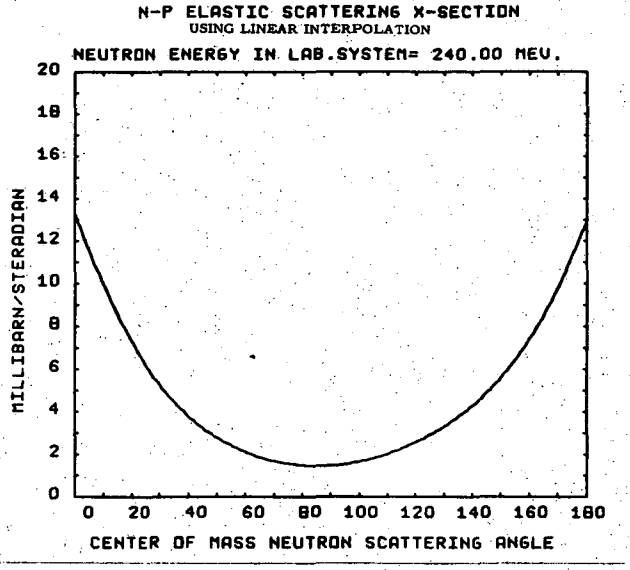

Fig. 40. Some examples of calculated np elastic scattering cross sections at some energies for which there are no experimental data.

TECHNICAL INFORMATION DIVISION
LAWRENCE RADIATION LABORATORY
UNIVERSITY OF CALIFORNIA
BERKELEY, CALIFORNIA 94720